Role of Quantum and Surface-State Effects in the Bulk Fermi-Level Position of Ultrathin Bi Films

T. Hirahara,[1,*] T. Shirai,[2] T. Hajiri,[3,†] M. Matsunami,[3] K. Tanaka,[3] S. Kimura,[3,‡] S. Hasegawa,[2] and K. Kobayashi[4]

[1]*Department of Physics, Tokyo Institute of Technology, Tokyo 152-8551, Japan*
[2]*Department of Physics, University of Tokyo, Tokyo 113-0033, Japan*
[3]*UVSOR Facility, Institute for Molecular Science, Okazaki 444-8585, Japan*
[4]*Department of Physics, Ochanomizu University, Tokyo 112-8610, Japan*

We performed high-resolution photon-energy and polarization-dependent ARPES measurements on ultrathin Bi(111) films [6–180 bilayers (BL), 2.5–70 nm thick] formed on Si(111). In addition to the extensively studied surface states (SSs), the edge of the bulk valence band was clearly measured by using S-polarized light. We found direct evidence that this valence band edge, which forms a hole pocket in the bulk Bi crystal, does not cross the Fermi level for the 180 BL thick film. This is consistent with the predicted semimetal-to-semiconductor transition due to the quantum-size effect [V.B. Sandomirskii, Sov. Phys. JETP 25, 101 (1967)]. However, it became metallic again when the film thickness was decreased (below 30 BL). A plausible explanation for this phenomenon is the modification of the charge neutrality condition due to the size effect of the SSs.

Bismuth (Bi) is an inevitable element in solid-state physics research. Many Bi-based compounds are investigated as superconducting cuprates [1] or topological insulators [2]. Pure Bi also shows exotic properties such as the unusually high diamagnetism [3] or valley polarization [4]. It is a semimetal with small hole and electron pockets. The Fermi wavelength is very long ($\sim$30 nm) and Bi has historically been studied in the quantum-size effects (QSE) of materials. For example, the oscillation of the film resistance with the thickness d was reported [5] and, furthermore, it was predicted that when the lowest quantum-well state (QWS) of the electron pocket is raised to an energy level higher than the highest hole subband in very thin films, a band gap opens [semimetal-to-semiconductor (SMSC) transition] at $d \sim 30$ nm [6]. Whether such a transition really occurs was debated [7] until it was realized that Bi has highly metallic surface states (SSs) [8]. The same SSs were also found in ultrathin Bi(111) films [9]. Because these SSs are spin split (the Rashba effect) [10–12], the interest shifted to measuring the SS conductivity [13–15]. The most favorable situation should be semiconducting bulk carriers due to the SMSC transition with metallic SSs in very thin films. *Ex situ* transport measurements on capped Bi films showed insulating property below $d \sim 90$ nm and a revival to a metallic one below 50 nm, interpreted as a SS contribution [16]. However, *in situ* magnetotransport measurements showed that Bi films thinner than 20 bilayers (BL; 1 BL = 0.39 nm) have both bulk and SS character, explained as a surface-bulk coherent transport [17]. So a direct observation of the precise bulk band dispersion is needed to clarify if the bulk is semiconducting or not in ultrathin Bi films.

In the present Letter, we performed high-resolution angle-resolved photoemission spectroscopy (ARPES) measurements to verify the change in energy position of the bulk band in ultrathin Bi(111) films. By tuning the photon energy ($h\nu$) and polarization, we observed the bulk valence band (that constitutes the bulk hole pocket) as well as the SSs. We have found direct evidence that this bulk state does not cross the Fermi level (E_F) for the 180 BL thick film, which is consistent with the SMSC transition. However, it unexpectedly became metallic again for thinner films (below 30 BL). A plausible explanation is the size effect of the SSs, which will change the Fermi surface and affect the bulk E_F to fulfill the charge neutrality condition of holes and electrons.

ARPES measurements were performed at BL-7U of UVSOR-III [18]. Two linearly polarized lights perpendicular and parallel to the mirror plane (S and P polarizations) can be irradiated to the sample without changing its position [19]. The total energy and angular resolutions were set at $\sim$15 meV and 0.16°, respectively. All of the measurements were performed at $\sim$20 K. Bi films (6–180 BL thick) were prepared on an n-type Si(111) substrate (P doped, $< 0.02~\Omega\,\mathrm{cm}$), as reported elsewhere [9,17,20,21].

First-principles calculations were performed using the WIEN2K computer code on the basis of the augmented plane wave plus local orbitals method taking into account the spin-orbit interaction [22], and the generalized gradient approximation [23] was used for the description of exchange-correlation potential.

Figure 1 shows the band dispersion along the $\bar{\Gamma} - \bar{M}$ direction taken at $h\nu = 15$ eV with P polarization for the 180 [Fig. 1(a)], 30 [Fig. 1(b)], 10 [Fig. 1(c)], and
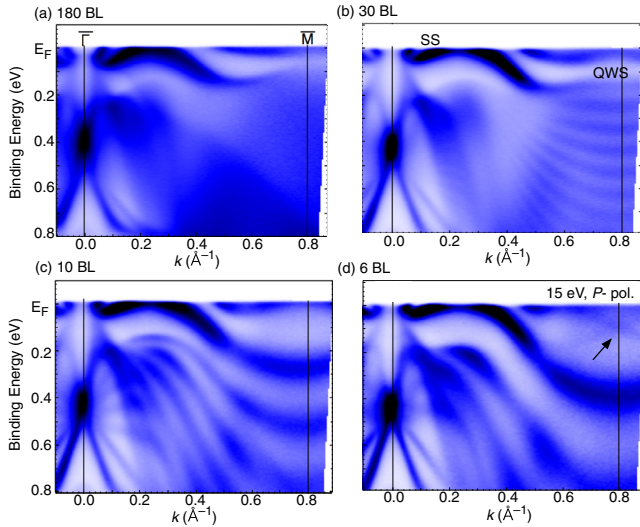
FIG. 1 (color online). Band dispersion of the 180 (a), 30 (b), 10 (c), and 6 (d) BL thick ultrathin Bi(111) films measured along the $\bar{\Gamma} - \bar{M}$ direction, respectively. The data were taken with P polarization at $h\nu = 15$ eV. SS and QWS correspond to surface and quantum-well states, respectively.

6 [Fig. 1(d)] BL thick Bi(111) films, respectively. The features near E_F is nearly thickness independent, composed of SSs. Below E_F, there is thickness dependence near $\bar{M}$ in Figs. 1(b)–1(d) for the thinner films, which are QWSs [9,24]. For the 180 BL thick film in Fig. 1(a), the QWSs are not observed since the energy spacing is too small. There are also some weak structures between the SS and the QWS in Fig. 2(d) (the arrow), which originate from the edge states [25]. The overall characteristics in Fig. 1 are the same as those reported previously [9,24,26,27].

The situation changes when the polarization of the incident photons is changed from P to S. Figure 2(a) shows the band dispersion for the 180 BL thick film measured at $h\nu = 15$ eV with S polarization. One can notice that the intensity of the SSs becomes drastically weak near $\bar{M}$, and the features near $\bar{\Gamma}$ have also changed.

Figure 2(b) shows an enlarged image of the region of the dotted rectangle in Fig. 2(a). In addition to the SSs, there is another feature which is located closer to $\bar{\Gamma}$. Ast and Höchst have identified this band as a bulk structure by changing $h\nu$ for a single crystal Bi(111) [8,28,29]. Figures 2(c) and 2(d) show the band dispersion measured at $h\nu = 18$ and 8 eV with S polarization, respectively, to show the $h\nu$ dependence for the 180 BL thick Bi film. Figure 2(e) compares the normal-emission ARPES spectra to see the $h\nu$ dependence quantitatively. The peak position remains at the same position (30 meV below E_F) irrespective of the incident light condition [30]. Because of quantization, it is a two-dimensional QWS. Since only one QWS is observed and to distinguish it from the QWSs in Fig. 1, we will call it "edge of the valence band" or "bulk edge (BE)." Compared to the spectrum of the metallic SS shown in the bottom of
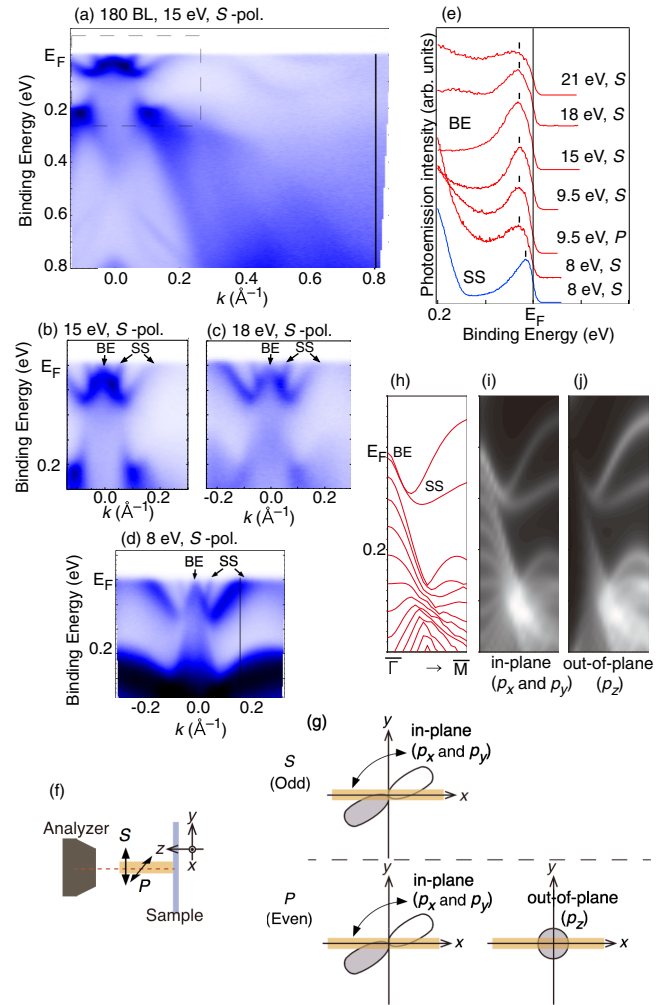
FIG. 2 (color online). (a) Band dispersion of the 180 BL thick Bi(111) film along the $\bar{\Gamma} - \bar{M}$ direction taken with S-polarized photons at $h\nu = 15$ eV. (b) Close-up of the region indicated by the dotted rectangle in (a). (c),(d) Same as (b) but taken at $h\nu = 18$ eV (c), and 8 eV (d), respectively. (e) Normal-emission ARPES spectra showing the bulk edge (BE) for the 180 BL thick Bi(111) film taken at different photon energies and polarizations. The last spectrum is that for the metallic surface states (SSs) taken at the solid line in (d). (f) Experimental geometry of the polarization-dependent ARPES. (g) Initial-state electronic orbital excited by polarized light at normal emission. The spatial symmetry of the p orbitals was oriented with respect to the mirror plane, and the orbitals were selectively excited with each polarization (S or P). The mirror plane including the direction of incidence and emission was defined along the x axis, as shown by the bold lines. (h) Calculated band dispersion of a 20 BL thick freestanding Bi(111) slab. (i),(j) The orbital components of the bands shown in (h) for the in-plane p_x and p_y orbitals (i), and the out-of-plane p_z orbital (j), respectively.

Fig. 2(e), it is clear that the BE is below E_F (semi-conducting). Since the bulk band at $\bar{\Gamma}$ crosses E_F for a single crystal Bi (Ref. [8]), our result is consistent with the SMSC transition prediction [6]. To the best of our knowledge, this is the first direct observation of the

semiconducting dispersion of the bulk valence band in Bi thin films. Although it was predicted that this happens at $d \sim 30$ nm [7], our measurements show that it happens in thicker films (180 BL ~ 70 nm), consistent with Ref. [16]. This discrepancy probably originates from the slightly different lattice constant between the film and the bulk [31] which was shown to alter the Bi electronic properties [32], or ambiguities in the theoretical models (boundary conditions and ignoring the SSs) [33].

Why is the BE observed clearly for S polarization, but not for P? Also, the SS intensity decreases dramatically in S polarization. This can be understood from symmetry analysis of the atomic orbitals that constitute the BE and the SSs. The photoemission intensity is expressed as $I \propto |\langle f|\mathbf{A} \cdot \mathbf{p}|i\rangle|^2 \delta(E_f - E_i - h\nu)$, where $\mathbf{A}$ and $\mathbf{p}$ are the vector potential and the momentum operator, and $|f\rangle$ (E_f) and $|i\rangle$ (E_i) are the final- and initial-state wave functions (energies), respectively. For normal emission [Fig. 2(f)], since the final state $|f\rangle$ has an even symmetry with respect to the mirror plane [34], the nonvanishing condition of the dipole transition $|\langle f|\mathbf{A} \cdot \mathbf{p}|i\rangle|$ is that the initial state $|i\rangle$ has the same symmetry (even/odd) as the dipole operator $\mathbf{A} \cdot \mathbf{p}$ [35,36]. Since the states near E_F of Bi are composed of $6p$ orbitals [37], we can say from our observation that the BE observed clearly with S polarization is only derived from the in-plane (p_x and p_y) orbital components, whereas the SSs are composed of both the in-plane and out-of-plane (p_z) orbitals [Fig. 2(g)].

We compare our findings with the *ab initio* calculation. Figure 2(h) shows the calculated band dispersion for a freestanding 20 BL thick Bi slab. Figures 2(i) and 2(j) show the mapping of the orbital components of the bands of Fig. 2(h) to the in-plane orbitals [Fig. 2(i)] and to the out-of-plane orbital [Fig. 2(j)], respectively. It can be seen that the BE is composed of the in-plane orbitals with little contribution from p_z, whereas the SS have a larger

weight on the p_z orbital. This is consistent with the above discussion [38].

Now let us discuss the thickness dependence of the BE. Figures 3(a) and 3(e) show the band dispersion for the 180 BL thick Bi(111) films measured at $h\nu = 9.5$ eV for P-[Fig. 3(a)] and S- [Fig. 3(e)] polarized photons, respectively. Both the SS and the BE are observed. For the films thinner than 30 BL, it is difficult to notice the BE (SS) by P-(S-) polarization [Figs. 3(b)–3(d) and 3(f)–3(h)]. We can say that the SS is observed by P-polarized photons, the BE by S-polarized photons. The important point is that the BE has moved above E_F [Figs. 3(f)–3(h)]. Thus, the bulk is again a (semi-)metal, which is the same as the single crystal Bi(111) [8]. Assuming a rigid band shift, the BE is now 20 meV above E_F [the dotted line in Fig. 3(h)]. This means that the BE shows a complicated thickness dependence: it is metallic for a bulk crystal, becomes semiconducting for $d = 180$ BL, and then becomes metallic again for $d < 30$ BL.

What is the origin of this behavior? As discussed above, the semiconducting band structure for the 180 BL thick film should be a consequence of the QSE [6]. In this scenario, the energy spacing between the QWSs should increase as the film thickness decreases and lead to an enhancement of the semiconducting energy gap. Nevertheless, we have observed that the BE becomes metallic again for thinner films. One possibility may be the charge transfer between the Si and the Bi. However, we did not observe any difference when Si substrates with different doping were used. Furthermore, there is a wetting layer that inhibits the substrate-film interaction [31]. Another possibility may be defect-induced doping, like in the case of topological insulators [2]. But since we do not observe a rigid SS band shift, this is also unlikely. We also believe that band bending effects cannot explain the experimental data since the film thickness is extremely small.
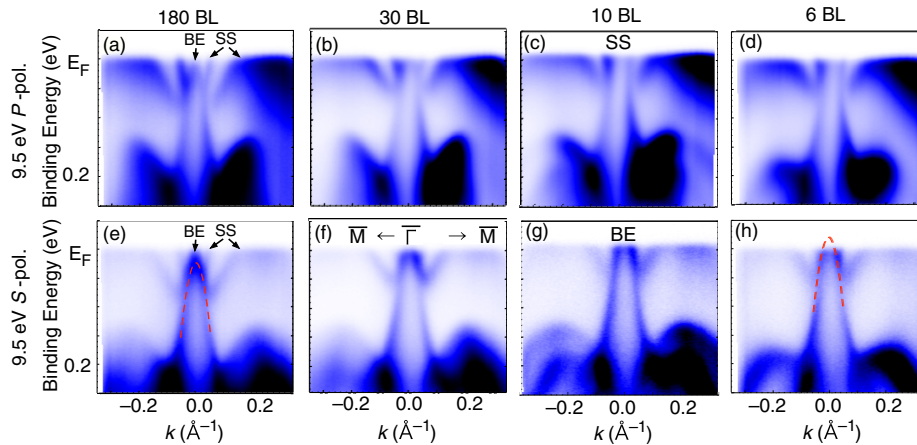
FIG. 3 (color online).   (a)–(d) Band dispersion of the 180 (a), 30 (b), 10 (c), and 6 BL (d) thick ultrathin Bi(111) films near the $\bar{\Gamma}$ point taken with P-polarized photons at $h\nu = 9.5$ eV, respectively. (e)–(h) Same as (a)–(d) but taken with S-polarized photons at $h\nu = 9.5$ eV. The red dotted lines in (e) and (h) indicate the approximate positions of the bulk edge (BE).
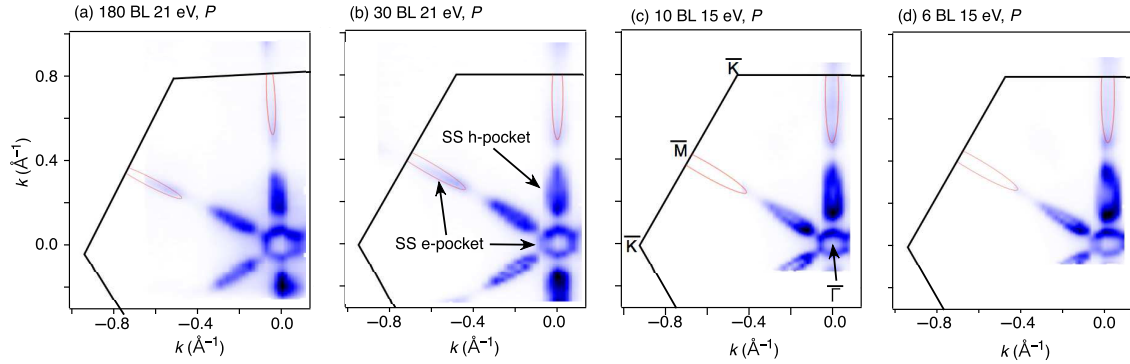
FIG. 4 (color online). Thickness dependence of the Fermi surface composed of the surface states (SSs) for the 180 (a), 30 (b), 10 (c), and 6 BL (d) thick Bi(111) films, respectively. The size of each pocket shows slight thickness dependence due to the side effect and induces change in the bulk Fermi level position.

One plausible explanation is the thickness dependence of the SSs. Figures 4(a)–4(d) show the measured Fermi surface of the Bi(111) ultrathin films for the 180 [Fig. 4(a)], 30 [Fig. 4(b)], 10 [Fig. 4(c)], and 6 BL [Fig. 4(d)] thick Bi(111) films, respectively. Although the basic features are the same with electron pockets around $\bar{\Gamma}$ and $\bar{M}$ and hole lobes along the $\bar{\Gamma} - \bar{M}$ direction, their size shows thickness dependence [39]. In particular, the sizes of the hole lobes and the electron pocket around $\bar{M}$ change. This is a result of the SS size effect; for very thin films, the top and bottom surfaces interact. This has been reported for Bi as a change in the spin polarization of the SS [10,26]. For ultrathin Bi_2Se_3 films, the SS band dispersion has been shown to be affected by this effect [40,41]. In the present case, the SS Fermi surface is modified associated with the band dispersion change and the electron-hole balance is affected [Figs. 4(b)–4(d)]. Table S1 shows the quantitative analysis of the carrier densities (see the Supplemental Material [42]). The 180 BL thick film shows nearly the same SS electron and hole concentrations, consistent with the single crystal case (Ref. [43]). However, the total SS electron carrier density is larger than the SS hole concentration for the thinner films. Therefore, additional hole carriers are needed and are supplied from the bulk. The estimated bulk hole carrier density is roughly consistent with the SS excess electron density (Table S1 [42]). The SSs were not considered in the simple SMSC transition prediction, and our results suggest that they can largely influence the bulk band position.

We note that *ab initio* calculations for freestanding Bi slabs have shown that the bulk valence band is more metallic for the thinner films [44]. Furthermore, the fact that both the bulk and the SSs are metallic for $d < 30$ BL is also consistent with the observed surface-bulk coherent transport [17]. Thus, the enhanced metallicity of the bulk hole pocket band with decreasing film thickness is confirmed by both experiment and theory.

In conclusion, we performed high-resolution photon-energy and polarization-dependent ARPES measurements on ultrathin Bi(111) films. In addition to the well-studied SSs, the bulk valence band edge was clearly observed. We found direct evidence of the valence band becoming semiconducting for the 180 BL thick film, which is consistent with the SMSC transition prediction. However, it became metallic again when the film thickness was decreased. A plausible explanation is the size effect of the SS, which can modify the charge neutrality condition and can change the bulk Fermi level.

[*]hirahara@phys.titech.ac.jp
[†]Present address: Department of Crystalline Materials Science, Nagoya University, Nagoya 464-8603, Japan.
[‡]Present address: Graduate School of Frontier Biosciences and Department of Physics, Osaka University, Suita 565-0871, Japan.

[1] P. A. Lee, N. Nagaosa, and X.-G. Wen, Rev. Mod. Phys. **78**, 17 (2006).
[2] M. Z. Hasan and C. L. Kane, Rev. Mod. Phys. **82**, 3045 (2010); X. Qi and S. Zhang, Rev. Mod. Phys. **83**, 1057 (2011).
[3] N. F. Mott and H. Jones, *The Theory of the Properties of Metals and Alloys* (Oxford University Press, New York, 1936).
[4] R. Küchler, L. Steinke, R. Daou, M. Brando, K. Behnia, and F. Steglich, Nat. Mater. **13**, 461 (2014).
[5] Yu. F. Ogrin *et al.*, JETP Lett. **3**, 71 (1966).
[6] V. B. Sandomirskii, Sov. Phys. JETP **25**, 101 (1967).

[7] C. A. Hoffman, J. R. Meyer, F. J. Bartoli, A. Di Venere, X. J. Yi, C. L. Hou, H. C. Wang, J. B. Ketterson, and G. K. Wong, Phys. Rev. B **48**, 11431 (1993); H. T. Chu, Phys. Rev. B **51**, 5532 (1995); C. A. Hoffman, J. R. Meyer, F. J. Bartoli, A. Di Venere, X. J. Yi, C. L. Hou, H. C. Wang, J. B. Ketterson, and G. K. Wong, Phys. Rev. B **51**, 5535 (1995).

[8] C. R. Ast and H. Höchst, Phys. Rev. Lett. **87**, 177602 (2001).

[9] T. Hirahara, T. Nagao, I. Matsuda, G. Bihlmayer, E. V. Chulkov, Y. M. Koroteev, P. M. Echenique, M. Saito, and S. Hasegawa, Phys. Rev. Lett. **97**, 146803 (2006).

[10] T. Hirahara, K. Miyamoto, A. Kimura, Y. Niinuma, G. Bihlmayer, E. V. Chulkov, T. Nagao, I. Matsuda, S. Qiao, K. Shimada, H. Namatame, M. Taniguchi, and S. Hasegawa, New J. Phys. **10**, 083038 (2008).

[11] A. Takayama, T. Sato, S. Souma, and T. Takahashi, Phys. Rev. Lett. **106**, 166401 (2011).

[12] T. Okuda, K. Miyamaoto, H. Miyahara, K. Kuroda, A. Kimura, H. Namatame, and M. Taniguchi, Rev. Sci. Instrum. **82**, 103302 (2011).

[13] T. Hirahara, I. Matsuda, S. Yamazaki, N. Miyata, S. Hasegawa, and T. Nagao, Appl. Phys. Lett. **91**, 202106 (2007).

[14] G. Jnawali, C. Klein, T. Wagner, H. Hattab, P. Zahl, D. P. Acharya, P. Sutter, A. Lorke, and M. Horn-von Hoegen, Phys. Rev. Lett. **108**, 266804 (2012).

[15] D. Lükermann, S. Sologub, H. Pfnür, and C. Tegenkamp, Phys. Rev. B **83**, 245425 (2011).

[16] S. Xiao, D. Wei, and X. Jin, Phys. Rev. Lett. **109**, 166805 (2012).

[17] M. Aitani, T. Hirahara, S. Ichinokura, M. Hanaduka, D. Shin, and S. Hasegawa, Phys. Rev. Lett. **113**, 206802 (2014).

[18] S. Kimura, T. Ito, M. Sakai, E. Nakamura, N. Kondo, T. Horigome, K. Hayashi, M. Hosaka, M. Katoh, T. Goto, T. Ejima, and K. Soda, Rev. Sci. Instrum. **81**, 053104 (2010).

[19] T. Hajiri, T. Ito, R. Niwa, M. Matsunami, B. H. Min, Y. S. Kwon, and S. Kimura, Phys. Rev. B **85**, 094509 (2012).

[20] T. Nagao, J. T. Sadowski, M. Saito, S. Yaginuma, Y. Fujikawa, T. Kogure, T. Ohno, Y. Hasegawa, S. Hasegawa, and T. Sakurai, Phys. Rev. Lett. **93**, 105501 (2004).

[21] S. Yaginuma, T. Nagao, J. T. Sadowski, A. Pucci, Y. Fujikawa, and T. Sakurai, Surf. Sci. **547**, L877 (2003).

[22] P. Blaha, K. Schwarz, G. K. H. Madsen, D. Kvasnicka, and J. Luitz, WIEN2K, *An Augmented Plane Wave+Local Orbitals Program for Calculating Crystal Properties* (Vienna University of Technology, Institute of Physical and Theoretical Chemistry, Vienna, 2001)

[23] J. P. Perdew, A. Ruzsinszky, G. I. Csonka, O. A. Vydrov, G. E. Scuseria, L. A. Constantin, X. Zhou, and K. Burke, Phys. Rev. Lett. **100**, 136406 (2008).

[24] T. Hirahara, T. Nagao, I. Matsuda, G. Bihlmayer, E. V. Chulkov, Y. M. Koroteev, and S. Hasegawa, Phys. Rev. B **75**, 035422 (2007).

[25] A. Takayama, T. Sato, S. Souma, T. Oguchi, and T. Takahashi, Phys. Rev. Lett. **114**, 066402 (2015).

[26] A. Takayama, T. Sato, S. Souma, T. Oguchi, and T. Takahashi, Nano Lett. **12**, 1776 (2012).

[27] G. Bian, T. Miller, and T.-C. Chiang, Phys. Rev. B **80**, 245407 (2009).

[28] C. R. Ast and H. Höchst, Phys. Rev. B **66**, 125103 (2002).

[29] C. R. Ast and H. Höchst, Phys. Rev. B **70**, 245122 (2004).

[30] We have confirmed that the peak position does not change for the photon energy of 7 to 21 eV in 0.5 eV steps for all films.

[31] T. Shirasawa, M. Ohyama, W. Voegeli, and T. Takahashi, Phys. Rev. B **84**, 075411 (2011).

[32] I. Aguilera, C. Friedrich, and S. Blügel, Phys. Rev. B **91**, 125129 (2015).

[33] H. T. Chu and W. Zhang, J. Phys. Chem. Solids **53**, 1059 (1992).

[34] The whole $\bar{\Gamma} - \bar{M}$ direction is included in the xz mirror plane.

[35] S. Hüfner, *Photoelectron Spectroscopy* (Springer, Berlin, 2003).

[36] R. Matzdorf, Surf. Sci. Rep. **30**, 153 (1998).

[37] Y. Liu and R. E. Allen, Phys. Rev. B **52**, 1566 (1995).

[38] One should also keep in mind that this selection rule is considered without including spin-orbit coupling. In general, spin-orbit coupling promotes an intermixing between odd and even symmetry bands, and thus the symmetry analysis does not strictly hold.

[39] In Ref. [24], it was mentioned that the SS Fermi surface shows little thickness dependence with slightly different Fermi wave numbers. The present data of Fig. 4 shows a much more clear thickness dependence. We believe this is due to the improved energy and angular resolutions, the lower sample temperature, and the smaller spot size of synchrotron radiation (smaller than 0.8 mm in both vertical and horizontal directions).

[40] Y. Sakamoto, T. Hirahara, H. Miyazaki, S. Kimura, and S. Hasegawa, Phys. Rev. B **81**, 165432 (2010).

[41] Y. Zhang *et al.*, Nat. Phys. **6**, 584 (2010).

[42] See Supplemental Material at http://link.aps.org/supplemental/10.1103/PhysRevLett.115.106803 for the quantitative analysis of the carrier density estimated from the size of the Fermi surface.

[43] C. R. Ast and H. Höchst, Phys. Rev. B **67**, 113102 (2003).

[44] Y. M. Koroteev, G. Bihlmayer, E. V. Chulkov, and S. Blügel, Phys. Rev. B **77**, 045428 (2008).